

# Q-ball formation in the gravity-mediated SUSY breaking scenario

S. Kasuya<sup>1</sup> and M. Kawasaki<sup>2</sup>

<sup>1</sup> *Department of Physics, Ochanomizu University, Bunkyo-ku, Tokyo 112-8610, Japan*

<sup>2</sup> *Research Center for the Early Universe, University of Tokyo, Bunkyo-ku, Tokyo 113-0033, Japan*  
(February 28, 2000)

We study the formation of Q-balls which are made of flat directions that appear in the supersymmetric extension of the standard model in the context of gravity-mediated supersymmetry breaking. The full non-linear calculations for the dynamics of the complex scalar field are made. Since the scalar potential in this model is flatter than  $\phi^2$ , we have found that fluctuations develop and go non-linear to form non-topological solitons, Q-balls. The size of a Q-ball is determined by the most amplified mode, which is completely determined by the model parameters. On the other hand, the charge of Q-balls depends linearly on the initial charge density of the Affleck-Dine (AD) field. Almost all the charges are absorbed into Q-balls, and only a tiny fraction of the charges is carried by a relic AD field. It may lead to some constraints on the baryogenesis and/or parameters in the particle theory. The peculiarity of gravity-mediation is the moving Q-balls. This results in collisions between Q-balls. It may increase the charge of Q-balls, and change its fate.

PACS numbers: 98.80.Cq, 11.27.+d, 11.30.Fs

hep-ph/0002285

## I. INTRODUCTION

A Q-ball is a kind of a non-topological soliton, whose stability is guaranteed by some conserved charge in scalar field theory [1,2]. It can be made of the scalar fields which appear as flat directions in the supersymmetric extension of the standard model [3,4]. Particularly, in the minimal supersymmetric standard model (MSSM), the baryon and/or lepton number are the conserved charges, since those flat directions consist of squarks and/or sleptons [5]. It is known that large Q-ball solutions exist when both gauge-mediated and gravity-mediated supersymmetry (SUSY) breaking scenarios are included [6,7]. In the gauge-mediation scenario, the baryonic charged Q-ball, the B-ball, is stable against decay into nucleons, since the energy per unit charge becomes less than the nucleon mass, 1 GeV, for large enough Q-ball charge:  $E \sim mQ^{3/4}$  [6]. Therefore, large B-balls can be a promising candidate for the cold dark matter. On the other hand, Q-ball energy grows linearly in the gravity-mediation scenario:  $E \sim mQ$  [8]. They can thus decay into both nucleons (baryons) and lightest supersymmetric particles (LSPs), which become the dark matter in the universe. In the both scenarios, we can expect a close relation between the energy density of the baryon and dark matter such as  $\Omega_b \sim \Omega_{DM}$  [6,8] ( $\Omega_b$  and  $\Omega_{DM}$  are density parameters of the baryon and the dark matter, respectively). In particular, a somewhat more definite relation on the number densities hold for the gravity-mediation scenario:  $n_{LSP} \simeq N_B f_B n_b$  [8,9]. Here  $N_B$  is the number of LSP decay products from the scalar field (flat direction) with unit baryon number, and  $f_B$  is the fraction of the charge stored in the form of Q-balls. For these mechanism to work, the charge of B-ball should be in the range  $10^{20} - 10^{30}$  [10,8].

Those large Q-balls are expected to be created through

Affleck-Dine (AD) mechanism [12] in the inflationary universe [6–8]. The coherent state of the AD scalar field which consists of some flat direction in MSSM becomes unstable and instabilities develop. These fluctuations grow large, and are expected to form into Q-balls. The formation of large Q-balls has been studied only linear theory analytically [6–8] and numerical simulations was done in one-dimensional lattices [6]. Both of them are based on the assumption that the Q-ball configuration is spherical so that we cannot really tell that the Q-ball configuration is actually accomplished. Some aspects of the dynamics of AD scalar and the evolution of the Q-ball were studied in Ref. [13], but the whole dynamical process was not investigated, which is important for the investigation of the Q-ball formation.

Actual Q-ball formation is confirmed in our recent work [14], where we showed the formation of Q-balls in the gauge-mediated SUSY breaking scenario using lattice simulations in one, two, and three dimensions in space. In that scenario, the typical size of Q-balls is determined by that of the most developed mode of linearized fluctuations when the amplitude of fluctuations grow as large as that of the homogeneous mode:  $\langle \delta\phi^2 \rangle \sim \phi^2$ . Almost all the initial charges which the AD condensate carries are absorbed into the formed Q-balls, leaving only a small fraction in the form of coherently oscillating AD condensate. Moreover, the actual sizes and the charges stored within Q-balls depend on the initial charge densities of the AD field. We also find that the evolution of the Q-ball crucially depends on its spatial dimensions, and the stable Q-ball can exist only in the form of three-dimensional object.

One may wonder if these results are peculiar to the gauge-mediation scenario which has a very flat scalar potential for the large field value. For a very flat scalar potential, larger Q-balls are easily formed, because the

energy of the Q-ball grows  $E \sim mQ^{3/4}$  [6]: the larger the charge is, the smaller the energy per unit charge is. On the other hand, the Q-ball energy grows linearly in the gravity-mediation scenario:  $E \sim mQ$  [8]. Thus, we naively expect less effective Q-ball formation, particularly for large charge Q-balls to form.

In this paper, we show the Q-ball formation in the gravity-mediation scenario by the use of numerical calculations. We find it very similar to gauge-mediation version, but some different new features are revealed.

In the next section, we see the origin of the fluctuations of the complex scalar field, and show the instability band. Results from numerical calculations are shown in Sec. III. Here the charge and the size of Q-balls are found. In Sec. IV, we will make some comments on the B-ball baryogenesis. We will show some peculiar phenomena of the Q-ball in the gravity-mediation scenario, such as the moving Q-balls, and their collisions as a result. Section VI is devoted to our summary and conclusions.

## II. INSTABILITIES OF AFFLECK-DINE CONDENSATE

Q-balls with large charge are expected to be formed through Affleck-Dine mechanism [6]. It is usually considered that the AD field is rotating homogeneously in its effective potential to make the baryon numbers. However, if we consider the SUSY-breaking included potentials, spatial instabilities of the AD field are induced by the negative pressure because of its potential being flatter than  $\phi^2$  [7,8,11]. To be concrete, let us take the following potential [7,8]:

$$V(\Phi) = m^2|\Phi|^2 \left[ 1 + K \log \left( \frac{|\Phi|^2}{M^2} \right) \right] - cH^2|\Phi|^2 + \frac{\lambda^2}{M^2}|\Phi|^6, \quad (1)$$

where  $\Phi$  is a complex scalar field which brings a unit baryon number,  $\lambda$  is a coupling constant of order unity,  $H$  is the Hubble parameter,  $c$  is a positive order one constant,  $M$  is a large mass scale which we take it as  $\simeq 2.4 \times 10^{18}$  GeV, and the  $K$ -term is the one-loop corrections due especially to gauginos, and the value of  $K$  is estimated in the range  $-0.01$  to  $-0.1$  [7,8]. In this potential, the pressure is estimated as [7]

$$P_\phi \simeq \frac{K}{2+K}\rho_\phi \simeq -\frac{|K|}{2}\rho_\phi, \quad (2)$$

where  $\rho_\phi$  is the energy density of the scalar field (Here we assume that  $|K| \ll 1$  so that the first term in Eq.(1) can be approximately rewritten in the power-law  $\phi^{2+2K}$ ). Therefore, the negative value of  $K$  is the crucial point for instabilities.

The homogeneous part of the field evolves as

$$\phi(t) \simeq \left( \frac{a_0}{a(t)} \right)^{3/2} \phi_0, \quad \dot{\theta}^2(t) \simeq m^2, \quad (3)$$

where we define the field  $\Phi$  to be

$$\Phi(t) = \frac{1}{\sqrt{2}}\phi(t)e^{i\theta(t)}. \quad (4)$$

Then the equations for the linearized fluctuations can be written as

$$\begin{aligned} \delta\ddot{\phi} + 3H\delta\dot{\phi} - \frac{1}{a^2(t)}\nabla^2\delta\phi - 2\dot{\theta}(t)\phi(t)\delta\dot{\theta} - \dot{\theta}^2(t)\delta\phi \\ + m^2 \left[ 1 + 3K + K \log \left( \frac{\phi^2}{2M^2} \right) \right] \delta\phi = 0, \\ \phi(t)\delta\ddot{\theta} + 3H[\dot{\theta}(t)\delta\phi + \phi(t)\delta\dot{\theta}] - \frac{\phi(t)}{a^2(t)}\nabla^2\delta\theta \\ + 2\dot{\phi}(t)\delta\dot{\theta} + 2\dot{\theta}(t)\delta\dot{\phi} = 0, \end{aligned} \quad (5)$$

We are now going to see the most amplified mode. To this end, we take the solutions in the form

$$\delta\phi = \left( \frac{a_0^2}{a^2(t)} \right)^{3/2} \delta\phi_0 e^{\alpha(t)+ikx}, \quad \delta\theta = \delta\theta_0 e^{\alpha(t)+ikx}. \quad (6)$$

If  $\alpha$  is real and positive, these fluctuations grow exponentially, and go non-linear to form Q-balls. Putting these forms into Eqs.(5), we get the following condition for the non-trivial  $\delta\phi_0$  and  $\delta\theta_0$ ,

$$\begin{vmatrix} F(H) + \ddot{\alpha} + \dot{\alpha}^2 + \frac{k^2}{a^2} + 3m^2K & -2\dot{\theta}\phi_0\dot{\alpha} \\ 2\dot{\theta}\dot{\alpha} & \left( \ddot{\alpha} + \dot{\alpha}^2 + \frac{k^2}{a^2} \right) \phi_0 \end{vmatrix} = 0, \quad (7)$$

where  $F(H) = -\frac{3}{2}\frac{\ddot{a}}{a} - \frac{3}{4}H^2$ .

It is appropriate to assume that  $H \ll m$  and  $\ddot{\alpha} \ll \dot{\alpha}$ , since the AD field oscillates when  $H \lesssim m$ , and the adiabatic production of fluctuations will occur. Then, Eq.(7) will be simplified as

$$\left( \dot{\alpha}^2 + \frac{k^2}{a^2} + 3m^2K \right) \left( \dot{\alpha}^2 + \frac{k^2}{a^2} \right) + 4\dot{\theta}^2\dot{\alpha}^2 = 0. \quad (8)$$

Since  $\dot{\theta}^2 \simeq m^2$ , for  $\dot{\alpha}$  to be real and positive, we must have

$$\frac{k^2}{a^2} \left( \frac{k^2}{a^2} + 3m^2K \right) < 0. \quad (9)$$

As we are considering  $K$  to be a negative value, an instability band will exist. This is because the oscillating scalar field in the potential flatter than  $\phi^2$  has negative pressure, which leads to the instability of the homogeneous field. Thus, the instability band should be in the range

$$0 < \frac{k^2}{a^2} < 3m^2|K|. \quad (10)$$

We can easily derive that the most amplified mode is the center of the band:  $(k_{max}/a)^2 \simeq 3m^2|K|/2$ , and it corresponds exactly to the Q-ball size which is estimated analytically using the Gaussian profile of the Q-ball [8]. We will see shortly that it also coincides with the size actually observed on the lattices in our simulations.

### III. CHARGE AND SIZE OF Q-BALLS

In this section, we show the results of the lattice simulations. In the potential (1), the AD field obeys the equation

$$\ddot{\Phi} + 3H\dot{\Phi} - \frac{1}{a^2}\nabla^2\Phi + m^2\Phi \left[ 1 + K + K \log\left(\frac{|\Phi|^2}{M^2}\right) \right] - cH^2|\Phi| + \frac{3\lambda^2}{M^2}|\Phi|^4\Phi = 0. \quad (11)$$

Here we have calculated in the matter-dominated universe, so that  $H = 2/3t$ . In the context of AD mechanism for baryogenesis, the A-terms, such as  $V_{A-term} \sim (A\lambda/M)\phi^4 + h.c.$ , should be added to the potential (1) in order to make the AD field rotate around in its potential. Instead, we take *ad hoc* initial conditions and neglect A-terms, since they do not affect the later dynamics of the field crucially. Therefore, the AD field possesses some initial charge density.

It is more convenient for numerical calculations to take the real and imaginary decomposition  $\Phi = (\phi_1 + i\phi_2)/\sqrt{2}$  and rescale as follows:

$$\varphi = \frac{\phi}{m}, \quad h = \frac{H}{m}, \quad \tau = mt, \quad \xi = mx. \quad (12)$$

For the initial conditions, we take some large vev in the real axis and put some angular velocity to the imaginary part. In addition, we put initial fluctuations very small values  $O(10^{-7})$ . Thus, they have the form

$$\begin{aligned} \varphi_1(0) &= A + \delta A(\xi), & \varphi_1'(0) &= \delta B(\xi), \\ \varphi_2(0) &= \delta C(\xi), & \varphi_2'(0) &= D + \delta D(\xi), \end{aligned} \quad (13)$$

where  $A$  and  $D$  are some constants, independent of the position in space,  $\delta A, \delta B, \delta C$ , and  $\delta D$  are  $\xi$  dependent small random variables, and the prime denotes the derivative with respect to  $\tau$ . Notice that the important features of the dynamics of the field are not affected by how we take these random variables, if we do not choose very peculiar distributions.

We have calculated the dynamics of the AD scalar field for various parameters, and find that the initially (approximately) homogeneous AD field deforms into a lot of clumpy objects. See Figs. 1 and 2. All of them conserve their charge very well, so they must be Q-balls. (We observed charge loss and exchange between two Q-balls in some cases. We will discuss them in Sect. V.) The profile of the Q-ball is a spherically symmetric thick-wall type, and fits very well to the Gaussian. In these figures,

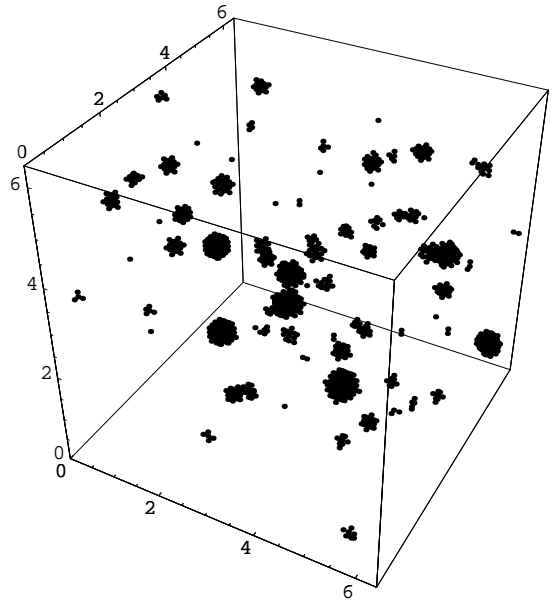


FIG. 1. Configuration of Q-balls on three-dimensional lattice. More than 40 Q-balls are formed, and the largest one has the charge with  $Q \simeq 5.16 \times 10^{16}$

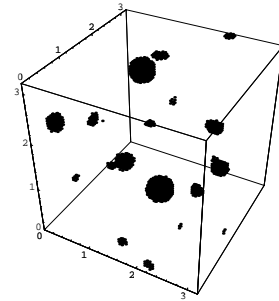


FIG. 2. Configuration of Q-balls on three-dimensional lattice. In each direction, the box size is half of that in Fig. 1. More than 10 Q-balls are formed, and the largest one has the charge with  $Q \simeq 1.74 \times 10^{16}$

we take  $\varphi_1(0) = \varphi_2'(0) = 2.5 \times 10^7$  for the initial conditions on the  $64^3$  three-dimensional (3D) lattices with  $\Delta\xi = 0.1$  and  $\Delta\xi = 0.05$  for the large and small lattice boxes, respectively. It seems that there is no box-size effects in these parameters, since these two figures look the same. They have similar charge distributions and the Q-ball size is the same, as expected from the analytical estimate,  $R_{phys} \sim |K|^{-1/2}m^{-1}$ . Actually, the numbers of Q-balls with the charge larger than  $10^{15}$  are 7 and 2 in the large and small box, respectively.

Comparing to those Q-balls which appear in the gauge-mediated SUSY breaking scenario, the size of the Q-ball is much smaller for the same charge, and most of the Q-balls has the same order of size. This is because  $R_{phys} \sim |K|^{-1/2}m^{-1}$  for the gravity-mediation, which does not depend on the charge  $Q$ , while  $R_{phys} \sim m^{-1}Q^{1/4}$  for the gauge-mediation. We thus observe large-charged Q-balls with relatively small size.

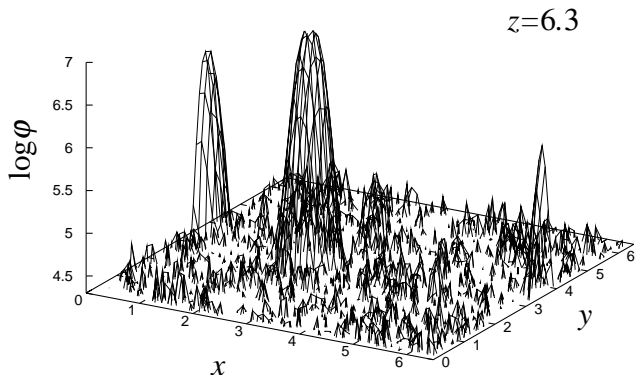


FIG. 3. Amplitude of the AD field after formation of Q-balls. This configuration is the slice at  $z = 6.3$ . The amplitude of relic field outside the Q-balls is two or three orders smaller than that of the center of the Q-balls.

As in the case of the gauge-mediation scenario [14], we observe almost all the charge which initially AD condensate has absorbed into Q-balls, and the amplitude of the relic AD field is highly damped. This means that the fraction of the charge outside Q-balls is very small. Figure 3 shows the amplitude of the AD field of the slice at  $z = 6.3$  in the larger box for another realization of simulations. Notice that there is relic field outside Q-balls, but the fluctuations are rather large, and we may not be able to consider it as a homogeneous condensate. In particular case of Figs. 1 and 2, Q-balls carry more than 97% and 99% of the total charge, respectively. In Fig. 4, the fraction of the charge outside the Q-balls is shown as a function of the number of Q-balls which we take into account. In the larger box simulation, only seven of the largest Q-balls hold more than 95% of the total charge. On the other hand, more than 97% is stored in only two of the largest Q-balls in the small box one. Notice that the dotted line (small box) is below the solid line (large box), because the resolution is twice as good in the former simulation: the lower bound is determined by the resolution of each simulations.

Analytically, some features of the Q-ball in gravity-mediation is known [8]. For example,

$$E \sim mQ, \quad R_{phys} \sim |K|^{-1/2} m^{-1}, \quad \omega \sim m, \quad \text{etc.} \quad (14)$$

They are all confirmed numerically. One example is shown in Fig. 5. This confirms the first relation of Eq.(14), which implies that the energy per unit charge is constant of  $O(m)$ .

It is the best way to investigate the dynamics of Q-ball formation on *three*-dimensional lattices, but it is practically difficult to do, since we need somewhat high resolution, and many runs for various parameters to look

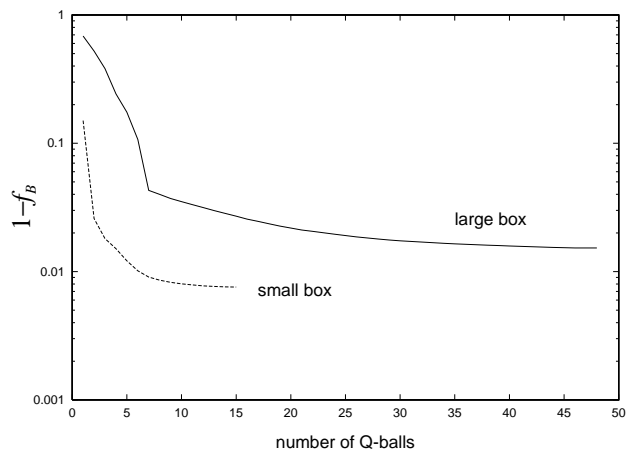


FIG. 4. Fraction of the charge outside the Q-balls. The solid and dotted lines denote the results from the simulations shown in Figs. 1 and 2, respectively.

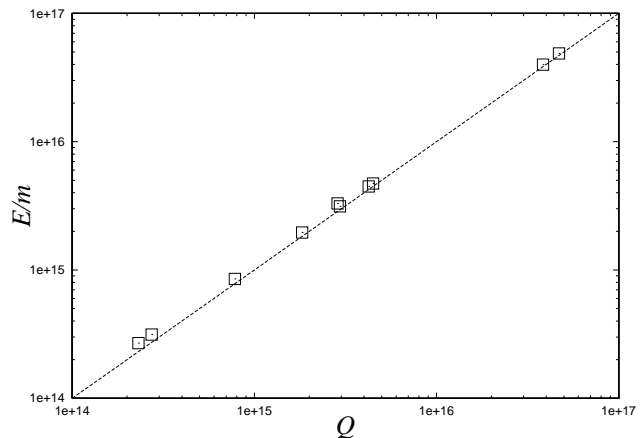


FIG. 5. Dependence of the energy of the Q-ball on its charge calculated on three-dimensional lattices. This confirms the analytical estimate:  $E \simeq mQ$  (the dotted line).

at. Thus, we also calculate on one and two-dimensional lattices for more rigorous quantitative analysis. Therefore, we must know the evolution of Q-balls after their formation. We follow the similar discussion we made for Q-balls in the gauge-mediation scenario [14]. Since a Q-ball configuration is the energy minimum with some fixed charge  $Q$ ,  $Q$  is constant with respect to time, so

$$Q = a^3 Q_D \sim a^3 R^D \tilde{q} \sim \text{const}, \quad (15)$$

where  $Q_D$  is the charge in  $D$  dimension, and  $\tilde{q} = \phi_1 \dot{\phi}_2 - \dot{\phi}_1 \phi_2$  is the charge density. If we assume the form of a Q-ball as

$$\phi(\mathbf{x}, t) = \phi(\mathbf{x}) \exp(i\omega t), \quad (16)$$

the energy of a Q-ball can be calculated as

$$E = \int d^3x \left[ \frac{1}{2} (\nabla \phi)^2 + V(\phi) - \frac{1}{2} \omega^2 \phi^2 \right] + \omega Q,$$

$$= \int d^3x [E_{grad} + V_1 + V_2] + \omega Q, \quad (17)$$

where

$$\begin{aligned} E_{grad} &\sim \frac{\phi^2}{a^2 R^2}, \\ V_1 &\sim m^2 M^{2|K|} \phi^{2-2|K|}, \\ V_2 &\sim \omega^2 \phi^2. \end{aligned} \quad (18)$$

Here we assume that the logarithmic term of the first term in the potential (1) is small compared to the unity, so that we can approximate it in the power-law form.

When the energy take the minimum value, the equipartition is achieved:  $E_{grad} \sim V_1$  and  $E_{grad} \sim V_2$ . From these equations addition to the charge conservation, we obtain the following evolutions:

$$\begin{aligned} R &\propto a^{-(1+2|K|)/[1+(D-1)|K|]}, \\ \phi &\propto a^{-(3-D)/[1+(D-1)|K|]}, \\ \omega &\propto a^{(3-D)|K|/[1+(D-1)|K|]}, \end{aligned} \quad (19)$$

which we observed approximately the same features numerically. For  $D = 3$ , we get very natural relations:  $R_{phys} = Ra \sim \text{const.}$ ,  $\omega \sim \text{const.}$ , and  $\phi \sim \text{const.}$  Although  $\phi$  decreases as time goes on for  $D = 1$  and 2,  $R$  and  $\omega$  is almost constant, since  $|K| \ll 1$ . This feature is different from that in the gauge mediation scenario, and is good for long simulations because low-dimensional Q-balls do not shrink the size so much.

Now we will see that the size of the Q-ball is determined by the most amplified mode. Comparing to the actual sizes observed on lattices, we also calculated numerically for linearized fluctuations. Although we decomposed the complex field in radial and phase direction in the previous section, it is more convenient to decompose it into real and imaginary part for numerical simulations. We thus integrated the following mode equations in dimensionless variables:

$$\begin{aligned} \delta\varphi_i'' + 3h\varphi_i' + \left[ \frac{k^2}{a^2} + 1 + K + K \log \left( \frac{\tilde{m}^2(\varphi_1^2 + \varphi_2^2)}{2} \right) \right. \\ \left. + 2K \frac{\varphi_i^2}{\varphi_1^2 + \varphi_2^2} - ch^2 \right. \\ \left. + \frac{3}{4} \lambda^2 \tilde{m}^2 (5\varphi_i^2 + \varphi_j^2)(\varphi_1^2 + \varphi_2^2) \right] \delta\varphi_i \\ + 2K \frac{\varphi_1\varphi_2}{\varphi_1^2 + \varphi_2^2} \delta\varphi_j = 0, \end{aligned} \quad (20)$$

where  $(i, j) = (1, 2), (2, 1)$ , and  $\tilde{m} = m/M$ .

Figure 6 shows the power spectrum calculated from a lattice simulation and the above linearized equations at  $\tau = 5.5 \times 10^3$  and  $\tau = 6 \times 10^3$ . We take the lattices with lattice size  $N = 1024$  and lattice spacing  $\Delta\xi = 0.1$  in one dimension here, because we need high resolution data to make the power spectrum smooth for lower  $k$ . These two times are just before and after the

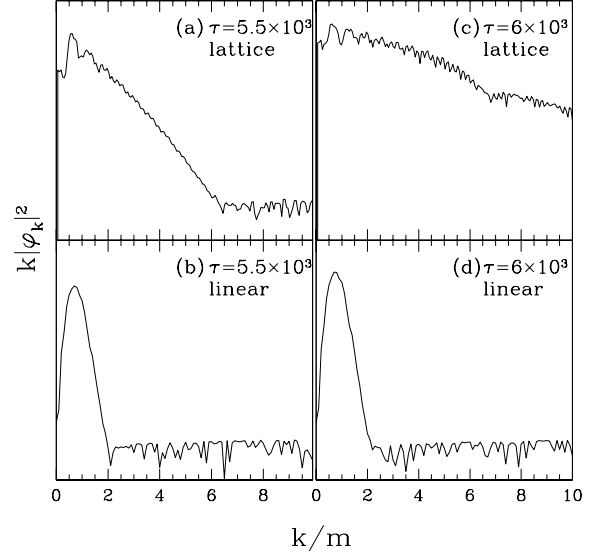


FIG. 6. Power spectra of fluctuations of AD scalar field ( $k^D |\delta\varphi_k|^2$ ,  $D = 1$ ) when the amplitude of fluctuations becomes as large as that of the homogeneous mode:  $\langle \delta\varphi^2 \rangle \sim \varphi^2$ . The top panels (a) and (c) show the full fluctuations calculated on one dimensional lattices, while the bottom panels (b) and (d) show the linearized fluctuations without mode mixing.

fluctuations are fully developed:  $\langle \delta\varphi^2 \rangle \sim \varphi^2$ . For linearized fluctuations, the instability band is almost the same as Eq.(10). For example, the upper bound is estimated by  $k/m = \sqrt{3}a(\tau)|K|^{1/2} \approx 2.5$  for  $|K| = 0.01$  and  $\tau = 5.5 \times 10^3$ . See panel (b). Even before the full development of fluctuations (panel (a)), rescattering effects kick the lower mode to higher, and the spectrum gets a little broader [15]. Needless to say, the spectrum becomes extremely broad and smooth after fluctuations are fully developed (panel (c)). At any times, however, the peaks are at the same points for both lattices and linearized cases, and correspond to the typical size of Q-balls actually observed on the lattices. Therefore, we can conclude that the size of the Q-ball is determined by the most amplified mode of the linearized fluctuations when they are fully developed. For the case of Fig. 6, the typical size is  $k_{max} \sim 0.5$ , which implies  $R_{phys} \sim a(\tau_f)/k_{max} \sim 28.9$ , where  $\tau_f \simeq 5.5 \times 10^3$  is the formation time. This value exactly coincides with the sizes of Q-balls observed on three-dimensional lattices. Actually, they are (a few)  $\times 10$  in the dimensionless units.

The actual values of the charge depend on the values of the charge density which AD field initially possesses. Since initial charge density is written as  $q(0) = \varphi_1(0)\varphi_2(0)$  for our initial conditions, we must check the dependence on both initial amplitude  $\varphi_1(0)$  and angular velocity  $\varphi_2'(0)$  of AD field. Results are shown in Fig. 7. Here we plot the largest charge  $Q_{max}$  against the initial AD charge density  $q(0)$ . We investigate two situations.

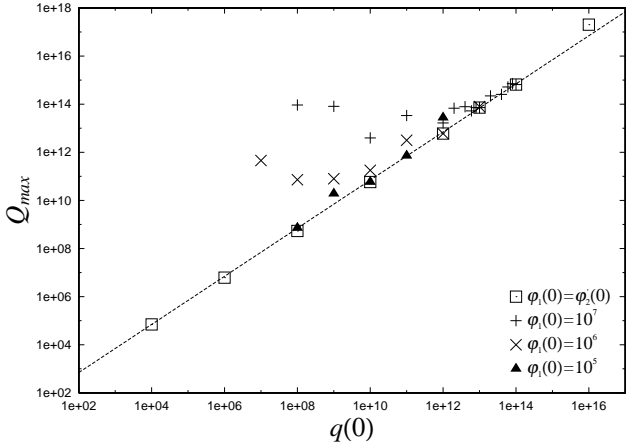


FIG. 7. Dependence of charges on the initial charge density  $q(0) = \varphi_1(0)\varphi_2'(0)$  carried by the AD condensate on one-dimensional lattices. Open squares denote the case  $\varphi_1(0) = \varphi_2'(0)$ , “pluses,” crosses, and solid triangles denote the dependence on  $\varphi_2'(0)$  with  $\varphi_1(0)$  fixed at  $10^7$ ,  $10^6$ , and  $10^5$ , respectively.

The first one is changing both equally while fixing the relation  $\varphi_1(0) = \varphi_2'(0)$ , which is shown by open squares in the figure. This corresponds to the “maximum charged” Q-balls in terms of Ref. [13]. We can fit all of these on the straight line (dotted line),  $Q_{max} \approx 7 \times q(0)$ , and the Q-ball charge depends linearly on the initial charge density.

The second situation is the dependence on the angular velocity  $\varphi_2'(0)$  while  $\varphi_1(0)$  is fixed. We calculate for three different value of  $\varphi_1(0)$ :  $10^7$ ,  $10^6$ , and  $10^5$ . In all cases, linear dependence is still preserved when the ratio of  $\varphi_1(0)$  and  $\varphi_2'(0)$  is within two orders of magnitude. However, if  $\varphi_2'(0)$  becomes smaller, the maximum Q-ball charge does not depend on the initial charge density. This is due to the creation of the negative-charged Q-balls. The charge is determined only by  $\varphi_1(0)$ .

Negative charge Q-balls are formed when the (initial) angular velocity is rather small. Figure 8 shows an example. In this case, we see the largest Q-ball with positive charge, two large negative charge Q-balls, and one Q-ball with positive charge an order of magnitude smaller for four largest ones. Similar situations occur in the gauge mediation scenario [14], but the critical value of the ratio  $\varphi_2'(0)/\varphi_1(0)$  for the negative charge Q-ball formation is larger in the gravity mediation scenario. This is because the angular motion of the AD condensate is more circular and stable, and the produced Q-ball size is larger in the flatter potential, so that it is more difficult to reverse the angular velocity of the field within that size.

In the actual situation, the AD field takes a very large vev before it rolls down to the origin of its potential, and the vev is determined by equating second and third terms in the potential (1):

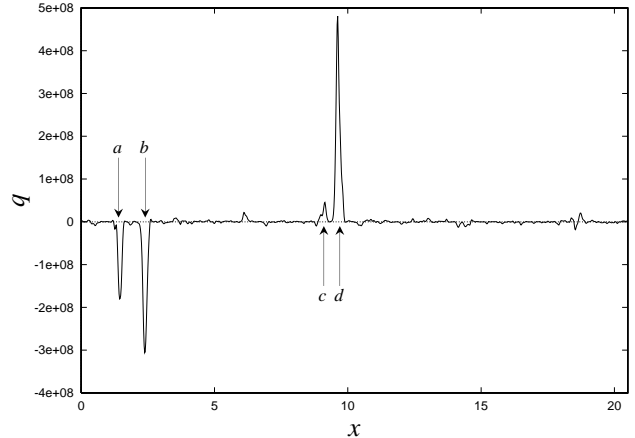


FIG. 8. Configuration of positive and negative Q-balls on one-dimensional lattice. Here we take  $\varphi_1(0) = 10^7$  and  $\varphi_2'(0) = 10^2$ . The four largest Q-balls have the charges (a)  $-2.9 \times 10^{13}$ , (b)  $-5.6 \times 10^{13}$ , (c)  $6.8 \times 10^{12}$ , and (d)  $8.1 \times 10^{13}$ .

$$\phi \sim \sqrt{\frac{HM}{\lambda}}. \quad (21)$$

The AD field begins to roll down when  $H \sim m$ , so its amplitude is  $\varphi \sim (\lambda\tilde{m})^{-1/2} \simeq 2.4 \times 10^7$  in the dimensionless parameters, where  $\tilde{m} = m/M$ . At the same time, the AD field begins rotation because of the A-term of the form,  $V_{A-term} \sim (\lambda m/M)\phi^4 + h.c.$  If we assume that the initial angular velocity is the same order as the initial amplitude in the dimensionless units, we get the initial charge density as  $q(0) = \varphi_1(0)\varphi_2'(0) \sim 6 \times 10^{14}$ . We expect the linear dependence between the initial charge density of the AD condensate and the produced largest Q-ball on three-dimensional lattices, as  $Q_{max} \simeq q(0) \times 10^2$ . This is shown in Fig. 9, where we take such initial conditions as the linear dependence is expected to hold, i.e.,  $\varphi_1(0) \sim \varphi_2'(0)$ . Using this relation, we can estimate the maximum charge of the actually expected Q-balls is  $Q_{max} \sim 6 \times 10^{16}$ . For the B-ball baryogenesis to work, the charge should exceed  $10^{20}$  [8]. Therefore, it may be a little difficult to reach this value in the parameters in the model. However, if we take  $\lambda^2\phi^{10}/M^6$  instead of  $\lambda^2\phi^6/M^2$  in the potential, as appears in the  $u^c d^c d^c$  flat direction [7,8], the initial vacuum expectation value (vev) of the AD field is estimated as  $\varphi \sim (\lambda\tilde{m}^3)^{-1/4} \simeq 7 \times 10^{10}$ . In this case, the initial AD charge density becomes  $\sim 5 \times 10^{21}$ , and it implies that the maximum Q-ball charge reaches as large as  $\sim 5 \times 10^{23}$ . Thus, we get enough value of the charge for B-ball baryogenesis.

#### IV. B-BALL BARYOGENESIS AND ITS RESTRICTIONS TO THE PARTICLE PHYSICS

As is known, baryon number and the amount of the dark matter can be directly related in the B-ball baryogenesis in the gravity-mediated SUSY breaking scenario [8].

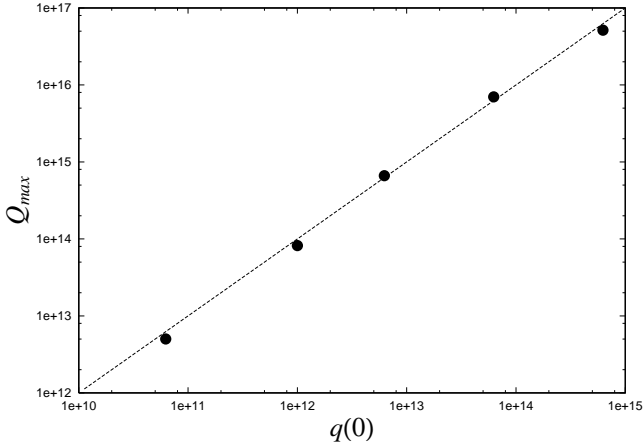


FIG. 9. Dependence of charges on the initial charge density  $q(0) = \varphi_1(0)\varphi_2'(0)$  carried by the AD condensate on three-dimensional lattices.

To this end, it is important to estimate how much charges are stored in the form of the Q-ball. In some cases, the fraction of the Q-ball charge may restrict the mass of the LSP, and vice versa [8,9]. We have calculated for various initial conditions on one-, two-, and three-dimensional lattices, and find that almost all the charges are absorbed into Q-balls. This fact is also true when we take other values for parameters in the potential. In particular, we investigate for the fraction of Q-ball charge, changing  $K$  from  $-0.01$  to  $-0.1$ . It was done by other method in Refs. [13], and they concluded that when the absolute value  $|K|$  was larger, the less the fraction. However, our results differ from theirs. We collect them in Tables I and II. The former is the results from one-dimensional lattices with the box size  $N\Delta\xi = 1024 \times 0.02 = 20.48$ . The latter table shows the results calculated in three dimensions. In this case, the box size is  $N\Delta\xi = 64 \times 0.1 = 6.4$ . As can be seen, the fraction of the sum of charge of Q-balls to the total charge has no dependence on the value of  $K$ . Moreover, neither does it depend upon the ratio of  $\varphi_1(0)$  and  $\varphi_2'(0)$ . All of them lead to a conclusion that almost all the charges are stored in Q-balls: that is,  $f_B \approx 1$ .

Following the argument of Refs. [8,9], the number density of the baryon to that of the dark matter ratio can be written in terms of density parameters as

$$\frac{n_b}{n_{DM}} = \frac{\Omega_b}{\Omega_{DM}} \frac{m_{DM}}{m_N}, \quad (22)$$

where  $m_N \simeq 1$  GeV is the nucleon mass. In the B-ball baryogenesis of the gravity-mediation scenario, B-balls decay into baryons and LSP neutralinos, so that the relation between the number density of baryon and dark matter is  $n_{DM} = N_B f_B n_b$ , where  $N_B$  is the number of neutralinos into which the AD field with a unit charge decays, and it is usually  $\gtrsim 3$ . Here we assume no later annihilation of neutralinos. Using the conservative constraint on the amount of the baryon number from the

TABLE I. Fraction of the charge stored in Q-balls for various values of  $K$  and  $\varphi_2'(0)/\varphi_1(0)$  on one-dimensional lattices.

$\varphi_2' \setminus K$	$-0.01$	$-0.05$	$-0.1$
$1.0 \times 10^7$	95.2%	98.6%	93.0%
$8.0 \times 10^6$	97.3	98.2	98.9
$6.0 \times 10^6$	98.0	99.9	99.7
$4.0 \times 10^6$	99.1	97.9	98.6
$2.0 \times 10^6$	99.0	97.6	98.3
$1.0 \times 10^6$	91.5	97.5	99.6
$8.0 \times 10^5$	97.6	95.5	97.0
$6.0 \times 10^5$	96.1	97.4	97.9
$4.0 \times 10^5$	99.4	95.2	99.7

TABLE II. Fraction of the charge stored in Q-balls for various values of  $K$  and  $\varphi_2'(0)/\varphi_1(0)$  on three-dimensional lattices.

$\varphi_2' \setminus K$	$-0.01$	$-0.05$	$-0.1$
$2.5 \times 10^7$	98.7%	99.7%	99.1%
$2.5 \times 10^6$	98.1	99.4	99.5
$2.5 \times 10^5$	98.4	99.8	99.2

Big-Bang nucleosynthesis,  $0.004 \lesssim \Omega_b h^2 \lesssim 0.023$  [17], we get a stringent constraint on the neutralino mass

$$7.1 \text{ GeV} \lesssim m_\chi \left( \frac{N_B}{3} \right) \left( \frac{\Omega_{DM} h^2}{0.49} \right)^{-1} f_B \lesssim 40.8 \text{ GeV}. \quad (23)$$

This bound is marginally consistent with  $f_B \approx 1$  and the accelerator experiment bounds such as  $M_\chi \gtrsim 24.2$  GeV [16]. Note that the constraint becomes more severe if  $\Omega_{DM}$  is smaller than 1 as in the case, for example, that considerable fraction of the total energy density is stored in the form of the cosmological constant [7,8]. In this case, the annihilation of neutralinos must be taken place.

## V. MOVING Q-BALLS, THEIR INTERACTIONS, AND BREATHER-LIKE SOLITON

As the consequence that the size of Q-balls is relatively small in the gravity-mediated SUSY breaking scenario, in a fixed volume, the coherent AD field breaks into larger numbers of Q-balls than in the gauge mediation scenario. Therefore, Q-balls can have somewhat large peculiar velocities, as opposed to Q-balls in gauge-mediation scenario. Actually, we observed moving Q-balls on the lattices in one, two, and three dimensions, but, unfortunately, Q-ball collisions (interactions) are observed only on one-dimensional lattices. This is not a surprise, since the impact parameter is small for small size Q-balls in two

or three dimensions. On the other hand, in one dimension, Q-balls must collide if they have enough (initial) velocities. We see the following three patterns for the interactions: (a) passing through, (b) exchanging part of charges, and (c) merging. They are expressed symbolically as

$$A + B \longrightarrow B + A, \quad (24a)$$

$$A + B \longrightarrow B' + A', \quad (24b)$$

$$A + B \longrightarrow C. \quad (24c)$$

These situations are plotted in Fig. 10. For the top three panels, they show the type (a), and two Q-balls with charges  $4.0 \times 10^{15}$  and  $1.8 \times 10^{15}$  are approaching, get together with the charge  $5.8 \times 10^{15}$ , and finally pass through each other without changing their own charges. For the middle three panels, they represent the type (b). They exchange about 10% of their charges. In the bottom three panels, we show the merging process.

Qualitatively, these processes can be divided by the relative velocity of two colliding Q-balls. If the relative velocity is large, they pass through each other without any (or negligible) charge exchange. When the velocity is smaller, two Q-balls exchange part of their charges. When the velocity is still slower, they merge into one, and it vibrates for a while. It can be a breather-like soliton, and an example is shown in Fig. 11. It repeats the double peaks and the single peak profiles just after the collision until it becomes stable state. During this process, we observed the decay of the charge by emitting very small Q-balls. For this particular example, about 7% of its charge is lost until it finally becomes stable and conserves its charge from that time on. The decrease of charge can be explained also by the emission of scalar waves, but we cannot distinguish them in the resolution of our simulations. In addition to the merging process (c), we see a few inverse processes: the breaking into two. These three processes (a), (b), and (c) are very similar to the results of Ref. [18], where the collision of non-topological solitons for other type is studied numerically on two-dimensional lattices. Although we do not have a chance to see any collision in two or three dimensions, their properties may be very similar if it happens to occur.

## VI. CONCLUSIONS

We have calculated the full non-linear dynamics of the complex scalar field, which represents some flat direction carrying the baryonic charge in MSSM, in the context of the gravity-mediated SUSY breaking scenario. Since the scalar potential in this model is flatter than  $\phi^2$ , we have found that fluctuations develop and go non-linear to form non-topological solitons, Q-balls. As in the gauge-mediation scenario [14], the size of a Q-ball is determined by the most amplified mode, but this mode is completely

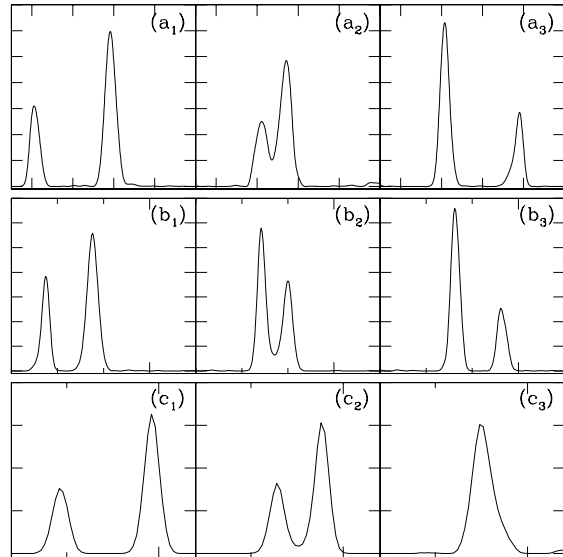


FIG. 10. Configurations of Q-balls for (a) passing through, (b) exchanging part of charges, and (c) merging.

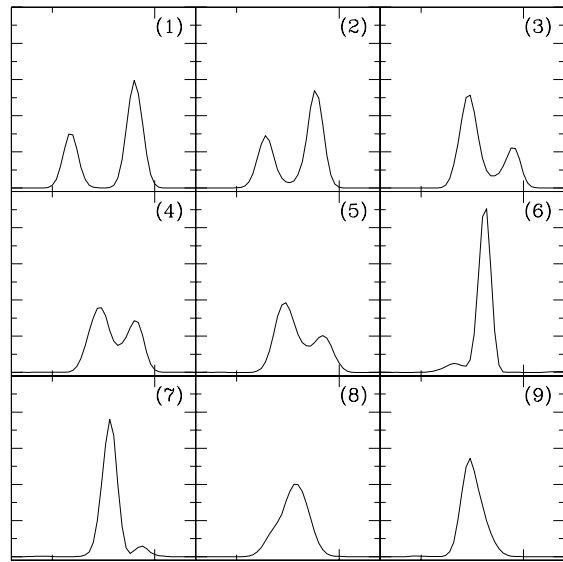


FIG. 11. Configurations of merging Q-balls on one-dimensional lattices. Each of the panels show the time snapshots at from (1)  $\tau = 4.375 \times 10^4$  to (9)  $\tau = 4.775 \times 10^4$  with the interval  $\Delta\tau = 0.05 \times 10^4$ .

determined by the model parameters  $m$  and  $K$ , and the size does not depend on the charge  $Q$ . On the other hand, the charge of Q-balls depends on the initial charge density of the Affleck-Dine field, and its dependence is linear. Therefore, large-charged Q-balls with relatively small size are formed in this scenario.

Once Q-balls are formed, almost all the charges are absorbed into them in all the simulations we made, and only a tiny fraction of the charge is carried by the relic



AD field, but its amplitude is very small and fluctuates so that it may not be possible to regard it as a condensate. This leads to some interesting results. We can restrict the scenario of the baryogenesis, which has a direct relation to the amount of the dark matter, or the parameter in MSSM, such as the neutralino mass, can be constrained.

We have also observed moving Q-balls, which is peculiar to the gravity-mediation scenario. In this case, larger numbers of Q-balls are formed in a fixed box size because of the relatively small Q-ball size, so the peculiar velocities are larger than those in the gauge-mediation scenario. As a consequence, there are collisions of Q-balls. The probability of collision crucially depends on the spatial dimensionality, and we have not found any collision in two or three dimensions. We thus expect the probability to be small in an actual situations. However, very interesting phenomena will occur, if collisions happen to take place. They are the charge exchange and merging to be large charge Q-balls. If the charge of a Q-ball becomes larger, it will be more difficult to evaporate or to be dissociated.

#### ACKNOWLEDGEMENT

M.K. is supported in part by the Grant-in-Aid, Priority Area “Supersymmetry and Unified Theory of Elementary Particles” (#707).

- 
- [1] S. Coleman, Nucl. Phys. **B262**, 263 (1985).
  - [2] A. Kusenko, Phys. Lett. **B404**, 285 (1997).
  - [3] A. Kusenko, Phys. Lett. **B405**, 108 (1997).
  - [4] G. Dvali, A. Kusenko, and M. Shaposhnikov, Phys. Lett. **B417**, 99 (1998).
  - [5] M. Dine, L. Randall, and S. Thomas, Nucl. Phys. **B458**, 291 (1996).
  - [6] A. Kusenko and M. Shaposhnikov, Phys. Lett. **B418**, 46 (1998).
  - [7] K. Enqvist and J. McDonald, Phys. Lett. **B425**, 309 (1998).
  - [8] K. Enqvist and J. McDonald, Nucl. Phys. **B538**, 321 (1999).
  - [9] K. Enqvist and J. McDonald, Phys. Lett. **B440**, 59 (1998).
  - [10] M. Laine and M. Shaposhnikov, Nucl. Phys. **B532**, 376 (1998).
  - [11] J. McDonald, Phys. Rev. **D48**, 2573 (1993).
  - [12] I. Affleck and M. Dine, Nucl. Phys. **B249**, 361 (1985).
  - [13] K. Enqvist and J. McDonald, Nucl. Phys. **B570**, 407 (2000).
  - [14] S. Kasuya and M. Kawasaki, Phys. Rev. **D61**, 041301 (2000).
  - [15] S.Yu. Khlebnikov and I.I. Tkachev, Phys. Rev. Lett. **77**, 219 (1996).
  - [16] C. Caso *et al.* (Particle Data Group), Eur. Phys. J. **C3**, 1 (1998).
  - [17] K.Olive, G. Steigman, and T. Walker, astro-ph/9905320.
  - [18] M. Axenides, S. Komineas, L. Perivolaropoulos, and M. Floratos, Phys. Rev. **D61**, 085006 (2000).